

Deletion at Fragile Sites Is a Common and Early Event in Barrett's Esophagus

Lisa A. Lai¹, Rumen Kostadinov⁵, Michael T. Barrett⁶, Daniel A. Peiffer⁷, Dmitry Pokholok⁷, Robert Odze⁸, Carissa A. Sanchez⁴, Carlo C. Maley⁵, Brian J. Reid^{2,3,4}, Kevin L. Gunderson⁷, and Peter S. Rabinovitch¹

Abstract

Barrett's esophagus (BE) is a premalignant intermediate to esophageal adenocarcinoma, which develops in the context of chronic inflammation and exposure to bile and acid. We asked whether there might be common genomic alterations that could be identified as potential clinical biomarker(s) for BE by whole genome profiling. We detected copy number alterations and/or loss of heterozygosity at 56 fragile sites in 20 patients with premalignant BE. Chromosomal fragile sites are particularly sensitive to DNA breaks and are frequent sites of rearrangement or loss in many human cancers. Seventy-eight percent of all genomic alterations detected by array-CGH were associated with fragile sites. Copy number losses in early BE were observed at particularly high frequency at FRA3B (81%), FRA9A/C (71.4%), FRA5E (52.4%), and FRA 4D (52.4%), and at lower frequencies in other fragile sites, including FRA1K (42.9%), FRAXC (42.9%), FRA 12B (33.3%), and FRA16D (33.3%). Due to the consistency of the region of copy number loss, we were able to verify these results by quantitative PCR, which detected the loss of FRA3B and FRA16D, in 83% and 40% of early molecular stage BE patients, respectively. Loss of heterozygosity in these cases was confirmed through pyrosequencing at FRA3B and FRA16D (75% and 70%, respectively). Deletion and genomic instability at FRA3B and other fragile sites could thus be a biomarker of genetic damage in BE patients and a potential biomarker of cancer risk. *Mol Cancer Res*; 8(8); OF1–11. ©2010 AACR.

Introduction

Barrett's esophagus (BE) is a condition in which the normal squamous lining of the esophagus is replaced by a metaplastic columnar (intestinal type) epithelium. BE develops in the context of chronic gastro-esophageal reflux disease, with repeated cycles of injury and repair in a genotoxic environment of exposure to acid, bile, and chronic inflammation (1, 2). BE is a premalignant condition—it is the only known precursor of esophageal adenocarcinoma (EA), a cancer that is increasing at an exponential rate in the United States. It is estimated that the incidence of gas-

tro-esophageal reflux disease within the population is ~10%; BE is estimated to develop in 10% of those individuals, and the annual incidence of EA in these patients is estimated to be 0.5% to 1% per year (3). BE is therefore of considerable clinical significance because the 5-year survival rate of EA is only ~10%, unless detected at an early stage, in which case it is curable. It is therefore recommended that BE patients be managed by endoscopic surveillance; however, at present, 95% of patients with EA do not have a prior diagnosis of BE (4). It is therefore important to define biomarkers that could be readily applied to patients with gastro-esophageal reflux disease to identify those who have BE and are at risk for EA, and would therefore benefit from endoscopic surveillance and/or medical or surgical intervention. Although conventional upper GI endoscopy has become widespread in its applications and availability, it is constrained by the requirement for patient sedation, as endoscopes large enough to allow biopsies are not otherwise tolerated (5). To address this problem, an accurate, sensitive molecular biomarker for the presence of BE would be of great utility.

Widespread genomic instability is believed to facilitate neoplastic progression in BE, as well as many other preneoplastic diseases. This process is facilitated by the loss and mutation of important cell cycle checkpoint machinery and tumor suppressor loci, such as p16 and p53. In addition, biomarkers of the process of genomic instability itself may be of clinical use. We have documented shortened

Authors' Affiliations: Departments of ¹Pathology, ²Medicine, and ³Genome Sciences, University of Washington, Seattle, Washington; ⁴Divisions of Human Biology and Public Health Sciences, Fred Hutchinson Cancer Research Center, Seattle, Washington; ⁵Molecular & Cellular Oncogenesis Program, Systems Biology Division, Wistar Institute, Philadelphia, Pennsylvania; ⁶Pharmaceutical Genomics Division, Translational Genomics Research Institute, Scottsdale, Arizona; ⁷Illumina, Inc., San Diego, California; and ⁸Department of Pathology, Brigham & Women's Hospital, Harvard Medical School, Boston, Massachusetts

Note: Supplementary data for this article are available at Molecular Cancer Research Online (<http://mcr.aacrjournals.org/>).

Corresponding Author: Peter S. Rabinovitch, University of Washington, Seattle, WA. Phone: 206-685-3761; Fax: 206-616-8271. E-mail: petersr@u.washington.edu

doi: 10.1158/1541-7786.MCR-09-0529

©2010 American Association for Cancer Research.

telomere length and chromosomal instability using fluorescence *in situ* hybridization in BE (6, 7). Although we have previously focused on sites of known tumor suppressors, we and others have shown that chromosomal “fragile sites” and, in particular, FRA3B, have an extremely high rate of deletion in BE patients (8, 9) and in patients that progress to EA (10). Thus, we hypothesize that fragile sites may serve as a sensitive biomarker of BE and the genotoxic injury that accompanies BE.

Fragile sites are loci that exhibit an increased propensity for sister chromatid exchange, translocation, and breaks under conditions of genotoxic stress (11, 12). The susceptibility of these loci to damage is believed to be a consequence of their primary and secondary structure, which affects chromatin organization and can stall DNA replication (13, 14). The resulting DNA gaps, breaks, and other chromosomal aberrations at fragile sites affect genomic stability, and often manifest as deletions and translocations. Currently, there are over 100 documented fragile sites within the human genome, categorized as “common” (present in all individuals) or “rare” (present in <5% of the population; refs. 13, 14); most are defined cytogenetically and their molecular characterization is not known.

Although instability at specific fragile sites has been linked to different cancers (15, 16) including breast (17), prostate, and lung (18, 19), there is still uncertainty about whether these fragile site alterations causally contribute to cancer development or are only “silent markers” of genomic stress. Putative tumor suppressors have been suggested to be located within common fragile sites; the fragile histidine triad gene, *FHIT*, at FRA3B and the WW domain–containing oxidoreductase, *WWOX*, at FRA16D have the best documented evidence for a role in cancer progression (20), whereas most other genes known to be at fragile sites, such as *parkin* at FRA6E, have less clear evidence for roles as tumor suppressors (21). Alternatively, breakage at fragile sites could contribute to repeated cycles of bridge-breakage-fusion, potentially promoting the amplification of oncogenes (22) such as *Met* within the FRA7G region (23) or the *prolactin-inducible protein (PIP)* gene (24).

We propose that as a consequence of chronic acid and nitric oxide exposure, and stalling the G₁-S transition in Barrett’s epithelium combined with impaired DNA repair pathways (25-28), there is an increased instability at fragile sites in this premalignant tissue. In previous studies of BE patients, copy number loss was detected at two fragile sites (FRA3B and FRA13B; refs. 8, 9). In this report, we include a larger sampling of new early-stage BE specimens and report genomic instability [copy number loss and/or loss of heterozygosity (LOH)] at many fragile sites in BE, some of which show increasing alterations with disease progression.

Materials and Methods

Patients and cells

All patients included in this study were participants in the Seattle Barrett’s Esophagus Study Program and were

evaluated as previously described (29). The endoscopic biopsies were analyzed for molecular alterations at chromosome arm 9p (*CDKN2A* locus), chromosome arm 17p (*TP53* locus), and DNA content tetraploidy and aneuploidy as previously described (29, 30). Two sets of patients were examined; genomic DNA was isolated from paired Barrett’s epithelium and gastric samples: (a) 20 patients without high-grade dysplasia characterized for chromosome arm 9p and/or 17p in which epithelial cells from selected biopsies were purified by Ki67/DNA content flow sorting. All biopsies were diploid by flow cytometry, measured as previously described (29). The maximum diagnoses for regions within 1 cm of biopsy site were as follows: six metaplasia, nine indefinite, and five low-grade dysplasia. Seven of the 20 patients were lost to follow-up; however, three of these patients progressed to low-grade dysplasia during surveillance. DNA content tetraploidy and aneuploidy was not detected in 19 of 20 of the baseline endoscopies. (b) Twenty patients with early molecular stage BE without chromosome arm 17p or DNA content tetraploidy or aneuploidy (Table 1) were analyzed by PCR and pyrosequencing, in which one to six biopsies (separated by a minimum of 2 cm longitudinally in the BE segment) were studied from each patient. Patients ranged in age from 36 to 81 years of age (mean, 60.8 y), and BE length ranged from 1 to 12 cm (mean, 5.7 cm). Biopsies were analyzed for molecular alterations at chromosome arm 9p (*CDKN2A* locus), chromosome arm 17p (*TP53* locus), and DNA content flow cytometry as previously described (29), and the maximum molecular abnormality for that patient is listed in Table 1. Histologic diagnosis was established by previously published criteria (29). All of the biopsies evaluated were within 1 cm of the maximum diagnosis as shown in Table 1. None of these patients overlapped with those examined previously by array-CGH (8).

Epithelial cells from these biopsies were purified by Ki67/DNA content flow sorting, and gastric cells were isolated by mincing of whole biopsy material as previously described. DNA was extracted using the Puregene DNA isolation kit (Invitrogen) as previously described (31). Cell lines from BE patients, CPA, CPB, CPC, and CPD, and their culture were as previously described (32, 33). The Seattle Barrett’s Esophagus Study has been approved by the Human Subjects Divisions of the University of Washington and/or the Fred Hutchinson Cancer Research Center continuously from 1983 to the present.

Agilent arrays

Genomic DNA. We obtained normal female 46, XX genomic DNA from Promega. The BE cell lines were maintained in modified MCDB 153 as previously described (33). In brief, genomic DNA was prepared from each cell line using the DNeasy Tissue kit (Qiagen). All DNA samples were gel verified for quality and assayed using a Nanodrop spectrophotometer to determine concentration and purity.

Table 1. Molecular and histologic data for samples analyzed by qPCR and pyrosequencing

Patient	Diagnosis	9p	17p	Aneuploid	Copy no. FRA3B	LOH FRA3B	Copy no. FRA16D	LOH FRA16D
1	Metaplasia	ND	ND	No	Gain	0 of 1	Normal	0 of 1
2	Metaplasia	No	No	No	Loss	2 of 4	Normal	3 of 4
3	Metaplasia	No	No	No	Loss	1 of 1	Normal	0 of 1
4	Metaplasia	No	No	No	Loss	1 of 1	Loss	1 of 1
5	Metaplasia	No	No	No	Loss	2 of 4	Loss	4 of 4
6	Metaplasia	No	No	No	Loss	0 of 1	ND	0 of 1
7	Metaplasia	No	No	No	Gain	1 of 1	Loss	1 of 1*
8	Metaplasia	No	No	No	Loss	1 of 1	Loss	1 of 1
9	Metaplasia	Yes	No	No	Loss	6 of 6	Normal	4 of 6
10	Metaplasia	Yes	No	No	Loss	0 of 1	Normal	1 of 1
11	Metaplasia	Yes	No	No	Loss	3 of 4	Loss	3 of 4
12	Indefinite	No	No	No	Normal	2 of 3	Normal	1 of 3
13	Indefinite	No	No	No	ND	2 of 2	ND	1 of 2
14	Indefinite	No	No	No	Loss	1 of 3	Normal	2 of 3
15	Indefinite	No	No	No	Loss	2 of 2	ND	1 of 2
16	Indefinite	Yes	No	No	ND	3 of 3	ND	3 of 3
17	Indefinite	Yes	No	No	Loss	1 of 1	Normal	1 of 1*
18	Low grade	Yes	No	No	Loss	2 of 2	ND	0 of 2
19	High grade	No	No	No	Loss	1 of 1	Loss	1 of 1
20	High grade	Yes	No	No	Loss	3 of 3	Normal	2 of 3

NOTE: For LOH, multiple sites were tested from patients, where available, relative to paired gastric constitutional. LOH reflects proportion of sites in which LOH or AI (see Materials and Methods) was detected relative to the total number of sites tested per patient. Copy number refers to qPCR data comparing the relative difference in copy number between the BE sample and the paired constitutional samples for one to two sites within the respective fragile sites normalized against two flanking sites.

Abbreviation: ND, not determined.

*LOH flank refers to LOH detected in genomic sequence flanking the fragile site, but not within FRA16D itself.

Sample labeling. For each CGH hybridization, 1 μ g of genomic DNA from the reference (46, XX female) and the corresponding experimental sample was digested with *AluI* (2.5 units) and *RsaI* (2.5 units; Promega). Labeling reactions were done directly with the restricted DNA and a Bioprime labeling kit (Invitrogen) according to the manufacturer's directions in a 50- μ L volume with a deoxynucleotide triphosphate pool to final concentrations of 120 μ mol/L dATP, 120 μ mol/L dGTP, 120 μ mol/L dTTP, 60 μ mol/L dTTP, and 60 μ mol/L Cy5-dUTP or Cy3-dUTP (Perkin-Elmer). Cell line samples were labeled with Cy5-dUTP and the reference sample with Cy3-dUTP in each experiment. Labeled targets were subsequently filtered using a Centricon YM-30 filter (Millipore). Experimental and reference targets for each hybridization were pooled, mixed with 50 μ g of human Cot-1 DNA (Invitrogen), and 100 μ g of yeast tRNA (Invitrogen) to a final volume of 250 μ L, then mixed with an equal volume of Agilent 2X *in situ* Hybridization Buffer.

Oligonucleotide microarray processing. Before hybridization to Agilent Human Genome 244K CGH arrays (Agilent Technologies), the 500- μ L hybridization mixtures were denatured at 100°C for 3 minutes and incubated at 37°C for 30 minutes. To remove any precipitate,

each mixture was centrifuged at $\geq 14,000 \times g$ for 5 minutes and transferred to a new tube, leaving a small residual volume ($\leq 5 \mu$ L). The sample was applied to the array using an Agilent microarray hybridization chamber, and hybridization was carried out for 40 hours at 65°C in a Robbins Scientific rotating oven at 20 rpm. The arrays were then disassembled and washed for 5 minutes at RT in wash 1 (0.5X saline-sodium phosphate-EDTA/0.005% NLS), followed by 3 minutes at 37°C in wash 2 (0.1X saline-sodium phosphate-EDTA/0.005% NLS). Slides were dried and scanned at 5- μ m resolution using an Agilent scanner. Image analysis was done using default CGH settings of Feature Extraction Software version 9.1 (Agilent Technologies).

ILLUMINA SINGLE NUCLEOTIDE POLYMORPHISM GENOTYPING

Paired constitutional and endoscopic BE samples were analyzed by the Illumina Infinium assay on high-density single nucleotide polymorphism (SNP) genotyping Bead Chips per manufacturer's instructions. In brief, genomic DNA was extracted from Ki67-positive flow-sorted epithelium samples as described or unsorted constitutive fundal mucosa from the lower esophageal sphincter or stomach. These samples underwent whole-genome amplification

using standard Infinium protocols. The resultant product was fragmented to ~500 bp by enzymatic digestion, precipitated, resuspended in hybridization buffer, denatured, and hybridized to the BeadChip overnight at 48°C. BeadChips were washed, primer extended, and stained on a Tecan Genesis/EVO robot using a Tecan GenePaint slide processing system. After staining, the BeadChips were washed, immediately coated with a protective reagent, and imaged on Illumina's BeadArray Reader. The image intensities are extracted, and the resultant data analyzed using the Illumina's BeadStudio 3.0 software.

The two types of SNP genotyping arrays used were as follows: HumanHap300 BeadChip (317k loci) and a noncommercial multisample HumanHap300_Pool 10 BeadChip (33k loci) that contained a subset (single beadpool) of the overall SNPs from the HumanHap300 BeadChip (33k) in a 12-sample format (32). Illumina HumanHap300 arrays were processed and scanned at the Children's Hospital of Philadelphia, and the Illumina Human-1 and Illumina multisample 33k BeadChips were processed at Illumina, Inc. All sample pairs were analyzed in "paired mode" using BeadStudio 2.0 or 3.0 as described (34).

Copy number estimates and genotype calls for Illumina BeadChips were calculated using the BeadStudio 2.0 output for raw intensity values and subsequent analyses. Log₂ intensity ratios for BE samples relative to paired constitutional controls were analyzed per patient for significant regions of copy number loss or gain using the Clustering among Chromosomes software (35) with a three-SNP moving window and a False Discovery Rate of 0.01. Copy number differences were manually curated to include only events with an average log₂ intensity ratio of >0.26 or <-0.32, corresponding to a minimum change of 20% between constitutional and test samples. Fragile site names and cytoband locations were downloaded from the National Center for Biotechnology Information MapViewer (Build 36.2; http://www.ncbi.nlm.nih.gov/mapview/map_search.cgi?taxid=9606). Cytoband positions were obtained from the University of California at Santa Cruz Genome Annotation Database (hg18; <http://hgdownload.cse.ucsc.edu/goldenPath/hg18/database/>). LOH was determined as a minimum of 20% difference in the relative allele frequency between the paired constitutional and BE samples in regions containing at least one informative SNP. Frequency *P* values for the all copy number loss, copy number gain, and LOH were evaluated for each chromosome arm using STAC v1.2 with data outputted in binary format per 1-Mb region and 500 permutations per analysis (36). A *P* value cutoff of 0.05 was used for selection of fragile sites with significant regions of loss.

Quantitative PCR

DNA was extracted from gastric or flow purified BE epithelium, and amplified with quantitative PCR using the Biotage Rotorgene RG-3000 using a protocol adapted from Boehm et al. (37). Initial DNA concentrations were measured using the Nanodrop ND-1000 and adjusted to 4

ng/μL. Cycle threshold was determined using a Sybr Green fluorescence threshold of 20%; copy numbers were estimated based on amplification relative to a standard curve (two-fold increments ranging from 0.25 to 4 ng) and prepared with pooled male genomic DNA (Promega #1471). One Cycle threshold difference equates to a loss of one gene copy. Individual runs were normalized against multiple genomic DNA control samples to facilitate comparison between reactions with varying efficiencies. Two primers located within region of loss (as determined by SNP genotyping) and one 5' and one 3' flanking primer set (on the same chromosome but at least 10-Mb from the fragile site) were used to compare copy number. Primer sequences are provided in Supplementary Table S1. Copy number estimates were evaluated per chromosome, with flanking regions normalized to two copies. The ratio between copy number for BE relative to gastric within the fragile site was then used to identify copy number gains (ratio, ≥1.2) or copy number loss (ratio, ≤0.8). All samples were run in triplicate.

Pyrosequencing

LOH at fragile sites was independently confirmed on 20 BE patients by SNP pyrosequencing. Patient data are summarized in Table 2; DNA from multiple sites at 2-cm intervals within a single BE segment was evaluated when material was available. For each patient, genomic DNA was extracted from flow-sorted endoscopic biopsies and unsorted gastric biopsies. Pyrosequencing (forward, reverse, and sequencing) primers were designed using the PSQ Assay Design 1.0 software to select primers with similar melting temperatures, with products ranging from 80 to 120 bp, and overall scores above 85. BLAT search (<http://genome.ucsc.edu/cgi-bin/hgBlat>) was used to confirm unique sequence for each PCR product. Primers selected to interrogate fragile site FRA3B (see Supplementary Table S1) had a mean HapMap minor allele frequency of 0.338, and FRA16D (see Supplementary Table S1) had a mean HapMap minor allele frequency of 0.299. PCRs were done using standard PCR protocol (1X PCR buffer, 1.5 mmol/L MgCl₂, 0.2 ng DNA, 5 mmol/L deoxynucleotide triphosphate, 5 μmol/L primers, 1.25 units AmpliTaq) and amplified using this program: 95°C, 4 minutes, then 45 cycles at 95°C, 15 seconds; 57°C, 30 seconds; 72°C, 15 seconds. Pyrosequencing reactions were purified over vacuum prep and mixed with sequencing primer as per manufacturer's instructions. All reactions were done on the Biotage PSQ HS 96. Allele frequencies were outputted as relative percentages using the Biotage PSQ software, and genotypes were assigned based on the relative allele frequency between constitutional and experimental samples. Informative calls were evaluated as relative ratios of 50:50 ± 10%. Allelic imbalance (AI) was assigned to SNPs, which were informative in the constitutional sample and showed relative allele frequencies of >66:33 to 89:11 in the BE sample. LOH was determined as ratios 90:10 or greater in the BE sample with an informative ratio in the constitutional sample.

Clustering analysis

Average copy number estimates for each fragile site region in Fig. 1A were analyzed in Cluster version 2 using complete linkage and hierarchical clustering with uncentered correlation. Heat maps were visualized using Tree-View version 1.60.

Results

Instability at multiple fragile sites detected in endoscopic BE samples

To examine whether copy number losses could be detected in fragile sites from early-stage BE clinical samples, genome-wide analyses were done using DNA isolated from 20 patients without high-grade dysplasia selected from the Seattle Barrett's Esophagus Surveillance Program. DNA extracted from diploid BE epithelium was Ki67/DNA content flow sorted and analyzed for genome-wide abnormalities using multisample Illumina 33K arrays relative to paired gastric constitutional DNA.

We first evaluated whether copy number alterations or LOH would be associated with alterations at predicted fragile sites defined solely by cytoband location because

most fragile sites are thus far uncharacterized. Copy number loss, copy number gain, and/or LOH were indeed detected in two or more patients at genomic regions associated with 56 different fragile sites (Fig. 1). Overall, copy number loss was detected at an average of 9.8 fragile sites per patient within this set, and 2 of the 20 patients showed copy loss at over 20 different chromosomal fragile sites. As shown in Fig. 1A (top), the most frequent and significant losses were observed at FRA3B (81%), FRA9A/9C (71.4%), FRA4D (52.4%), FRA5E (52.4%), FRA1K (42.9%), FRAXC (42.9%), FRA16D (33.3%), and FRA12B (33.3%). Note that although there was no coverage for p16/CDKN2A on the 33K arrays, we believe that the deletion observed in the region of FRA9A/9C was likely at p16/CDKN2A, consistent with earlier reports that this locus is frequently mutated or deleted in BE. The regions of deletion seen in fragile sites FRA3B and FRA16D were surprisingly small and consistent; the consensus regions of copy change being 400 and 230 kb, respectively. The compact nature of these changes is further illustrated in Figs. 2 and 3.

On average, copy gain was present at an average of 4.5 fragile sites per patient (Fig. 1A, middle). Individual sites of

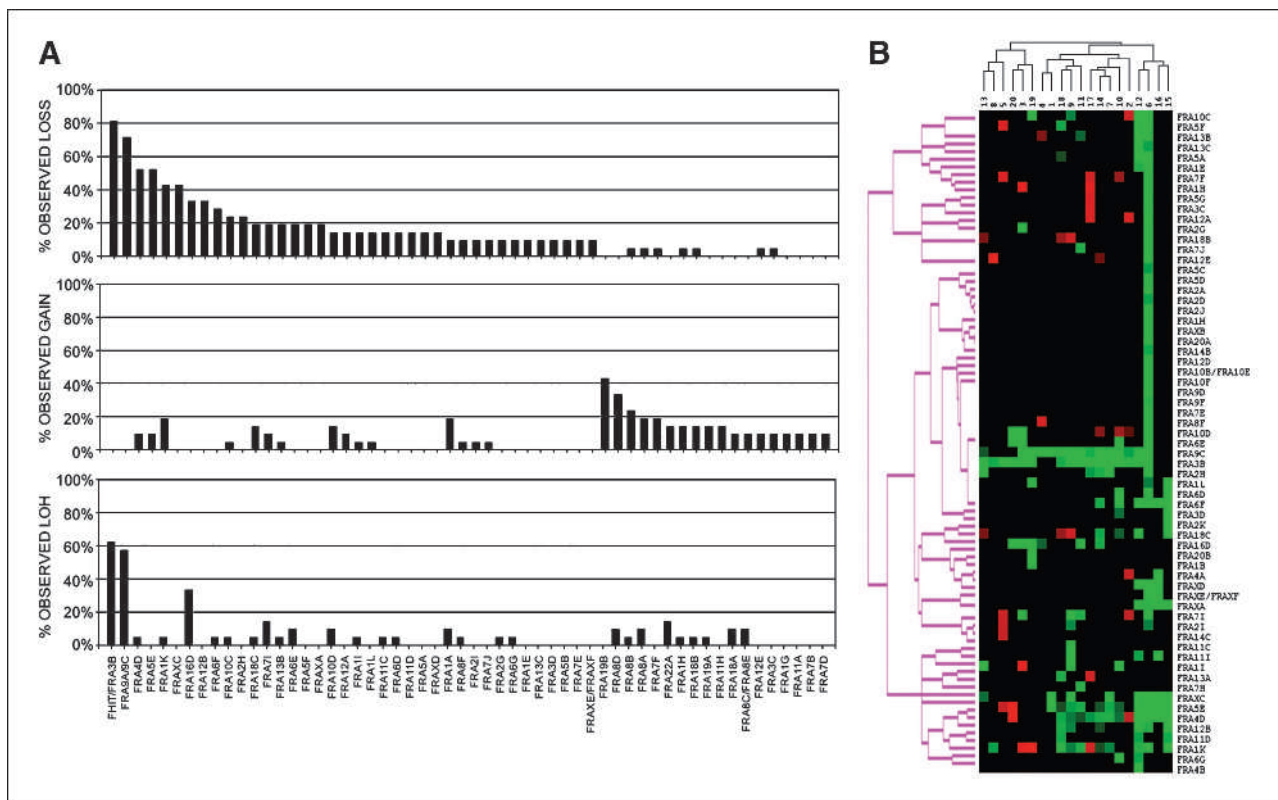


FIGURE 1. Copy loss, copy gain, and LOH at fragile sites in BE samples. A, shown is frequency of copy number loss (top), copy number gain (middle), or LOH (bottom) within the respective cytoband regions for fragile sites with alterations in two or more patients. Copy number changes were determined using the CGH-Miner software, and LOH was determined using the relative allele frequency between the BE sample and the paired constitutional sample. B, clustering analysis for fragile site copy number gain and loss by patient. Black, normal copy number; red, copy gain; green, copy loss for individual fragile sites.

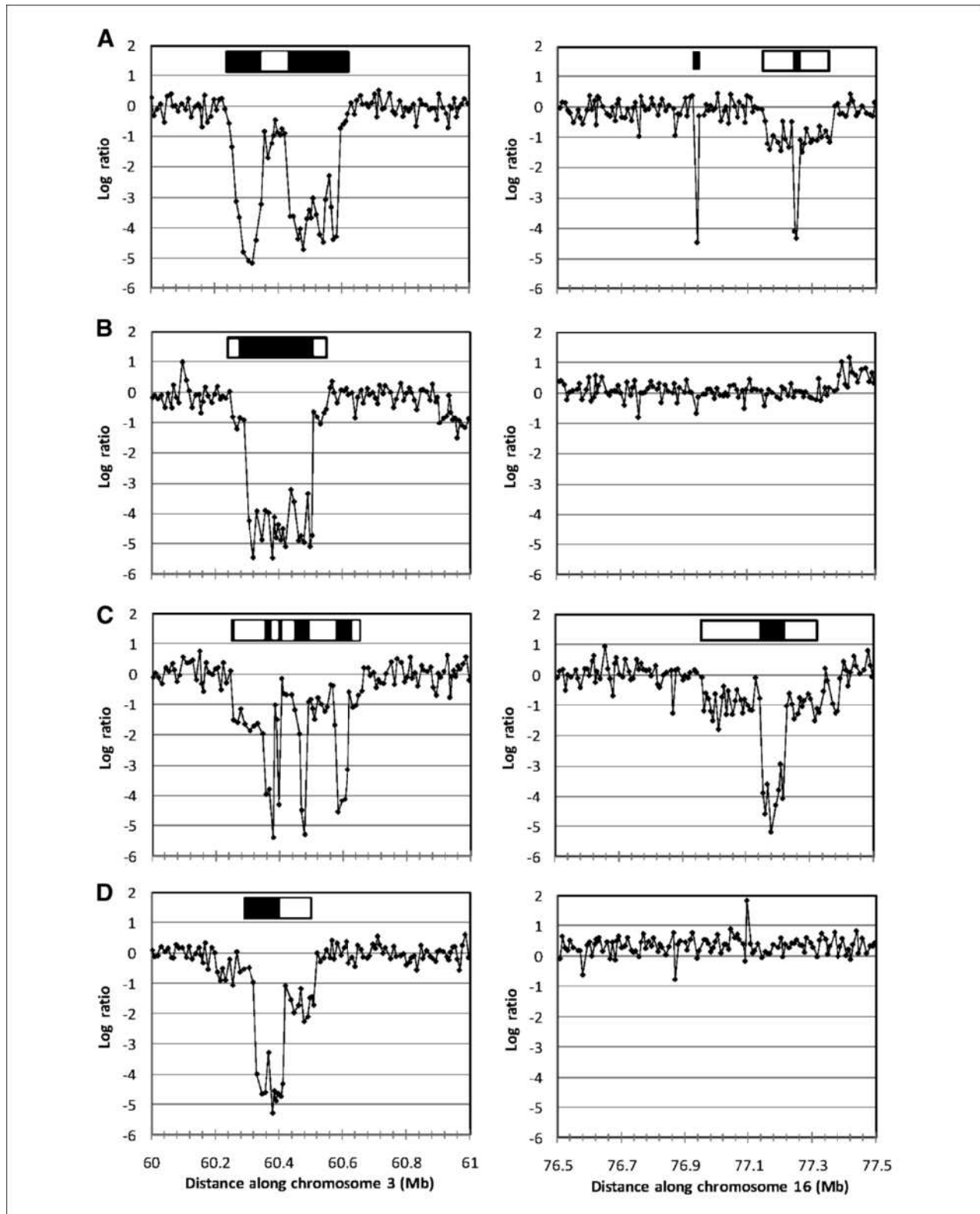


FIGURE 2. Copy number loss at common fragile sites detected in BE cell lines. Copy number plots showing FRA3B (left) and FRA16D (right) for individual BE cell lines (A, CPA; B, CPB; C, CPC; D, CPD) analyzed on Human Genome (244K) arrays. A log ratio of -1 represents one-copy number loss, and a \log_2 ratio of ~ -4 corresponds to homozygous two-copy number loss in at least 95% of cells. Open and closed boxes above each plot, approximate extents of one- and two-copy number loss, respectively.

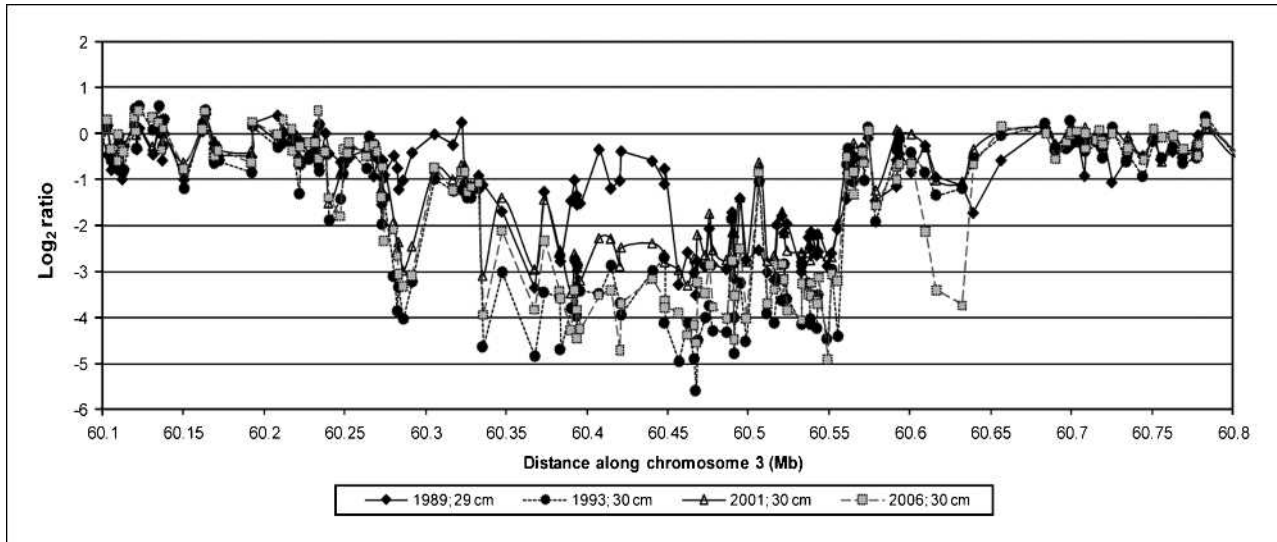


FIGURE 3. HumanHap300 (317k) array analysis of BE biopsies at the same level (± 1 cm) from one patient over four endoscopies from 1989 to 2006. \blacklozenge , 1989; \bullet , 1993; \blacktriangle , 2001; \blacksquare , 2006. In 1989, the BE consensus FRA3B region showed a region of one-copy number loss (b) flanked by two-copy number loss (a), with an adjacent region of one-copy number loss (c). In 1993, a and b merged into a region of uniform two-copy number loss (f), flanked by new regions of two-copy (d) and one-copy (e) loss. In 2006, the region of one-copy number loss at c lost its second copy (g).

gain were observed at low frequency except at FRA19B (42.9%), FRA8D (33.3%), and FRA8B (23.8%). LOH was observed at an average of 2.6 sites per patient (Fig. 1A, bottom) and was detected at higher than expected frequency in three fragile sites, FRA3B (61.9%; $P = 0.002$), FRA9A/9C/p16/CDKN2A (57.1%; $P = 0.002$), and FRA16D (33.3%; $P = 0.002$). However, the total number of LOH calls made with the 33K arrays may be underestimated, as the lower number of informative SNPs on these arrays reduces the ability to detect small regions of LOH compared with determination of copy change, which is based on all 33K probes.

Figure 1B illustrates a clustering analysis of patients showing copy number gain or loss at individual fragile sites; the highest correlation was detected for losses at FRA3B and FRA9A/9C/p16/CDKN2A. We observed that a subset of patients (patient #6, 12, 15, and 16) had copy number loss detected at several fragile sites including FRAXC, FRA5E, FRA4D, FRA12B, FRA11D, and FRA1K, although interestingly, the most frequent copy number losses at FRA3B/FHIT and FRA9A/9C/p16/CDKN2A were not detected in patients 15 and 16. The most striking copy number losses were observed for patient #6. Future studies that correlate clusters of fragile site instability with patient outcome should be revealing; however, that information was unavailable for the majority of this patient set.

Because most fragile sites are uncharacterized, we asked whether conserved copy number and genotypic alterations could be detected in more defined regions within the cytobands; therefore, we used the frequency and footprint analysis of the Significance Testing for Aberrant Copy number (STAC) algorithm as described by Diskin et al. (36). We

postulated that if the fragile site instability were a consequence of the shared environment of inflammation and oxidative stress created in BE and enriched in specific DNA sequences, then conserved regions of copy number change should be detectable among our patient set. Results of the STAC analysis are shown in Table 2, which displays the subset of the fragile sites at which copy number losses, copy number gains, or LOH were statistically significant by this method. Seventeen regions of copy loss, gain, or LOH were identified within putative fragile sites. Moreover, there were an additional 10 regions of copy number loss, gain, or LOH located within 10 Mb of cytoband regions previously identified as fragile sites (Table 2, middle). These 27 regions in or near fragile sites represented 78.1% of all genomic alterations identified by STAC analysis as significantly altered in these 20 paired patient samples. Significant copy gain events were detected at FRA 8D, FRA11H, FRA19B, and FRA22A. A part of all SNPs detected as having LOH on the Illumina 33K arrays (29.5%) were located within just three fragile site regions, FRA3B, FRA9A/9C/p16/CDKN2A, and FRA16D.

Fragile site copy loss and LOH in early molecular stages of BE confirmed by q-PCR and pyrosequencing

To confirm the results observed by SNP genotyping, copy number and LOH were evaluated at two fragile sites using quantitative PCR (q-PCR) and pyrosequencing in 20 BE patients selected as having the earliest molecular stage of disease: without LOH on chromosome arm 17p and without DNA content tetraploidy and aneuploidy (30). Patient and biopsy information is provided in Table 1. For each case, DNA isolated from a BE biopsy that was Ki67/DNA content flow sorted was compared with a

Table 2. Regions of copy change and LOH

Alteration(s)	Cytoband(s)	Start (Mb)	End (Mb)	Fragile site	Type	Distance to fragile site	Frequency	Frequency <i>P</i>	Footprint <i>P</i>
Cloned fragile sites									
Copy loss	3p14.2	59	62	FRA3B	Common		80.00%	0.001	0.004
Copy loss	18q22.1	63	66	FRA18C	Rare		35.00%	0.001	0.004
Copy loss	16q23.3-24.1	76	78	FRA16D	Common		35.00%	0.001	0.004
Copy loss	7q31.2	117	118	FRA7G	Common		20.00%	0.001	0.002
LOH	3p14.2	59	61	FRA3B	Common		60.00%	0.001	0.002
LOH	16q23.3-24.1	77	79	FRA16D	Common		35.00%	0.001	0.002
Associated with fragile sites									
Copy loss	9p21	21	23	FRA9A/9C	Rare		75.00%	0.001	0.01
Copy loss	5p14	23	30	FRA5E	Common		55.00%	0.001	0.004
Copy loss	4p15	33	36	FRA4D	Common		45.00%	0.001	0.004
Copy loss	5p13	29	30	FRA5A	Common		45.00%	0.001	0.004
Copy loss	Xq22.1	98	99	FRAXC	Common		35.00%	0.01	0.01
Copy loss	1q31	185	187	FRA1K	Common		30.00%	0.001	0.01
Copy loss	12q21.3	81	85	FRA12B	Common		30.00%	0.01	0.002
Copy loss	10q21	67	69	FRA10C	Common		15.00%	0.07	0.01
Copy gain	8q24.3	144	146	FRA8D	Common		25.00%	0.39	0.01
Copy gain	19p13	0	5	FRA19B	Rare		35.00%	0.01	0.01
LOH	9p21	21	23	FRA9A/9C	Rare		55.00%	0.001	0.01
Near fragile sites									
Copy loss	5q14.3	83	90	(FRA5B/5D)	Common	1.9 Mb	50.00%	0.001	0.004
Copy loss	3q25-26.1	163	170	(FRA3D)	Common	1.8 Mb	45.00%	0.001	0.004
Copy loss	13q31.1	81	86	(FRA13B)	Common	9.9 Mb	40.00%	0.001	0.004
Copy loss	11p13	38	39	(FRA11E)	Common	1.6 Mb	35.00%	0.03	0.004
Copy loss	7q21.11	84	86	(FRA7E)	Common	4.9 Mb	35.00%	0.001	0.002
Copy loss	6q21	101	104	(FRA6F)	Common	0.8 Mb	30.00%	0.05	0.01
Copy loss	7p22	9	11	(FRA7B)	Common	1.8 Mb	20.00%	0.02	0.01
Copy loss	11q22.1	97	98	(FRA11F)	Common	8.1 Mb	20.00%	0.01	0.004
Copy loss	11q14.2	89	90	(FRA11F)	Common	1.1 Mb	20.00%	0.01	0.004
Copy gain	10q26.3	134	135	(FRA10F)	Common	6 Mb	15.00%	0.02	0.03
Nonfragile sites									
Copy loss	Xp21.1	31	33				45.00%	0.001	0.01
Copy loss	3p12.1	83	87				40.00%	0.001	0.004
Copy loss	Xq25	125	126				40.00%	0.003	0.01
Copy loss	6q22.31	124	125				35.00%	0.003	0.004
Copy loss	21q21.1	20	22				25.00%	0.01	0.04
Copy gain	9q34.2	135	138				20.00%	0.001	0.004
Copy gain	20q13.33	60	61				20.00%	0.01	0.002

NOTE: Shown are significant regions of copy number loss or LOH. Regions within cloned fragile sites (top set), associated with fragile sites (second from top), near fragile sites (within 10 Mb, third from top), or at nonfragile sites (bottom set) are shown. Cytogenetic band locations and the chromosome positions (start and end) are noted; the latter indicates the largest extent of the chromosomal region identified by STAC as being statistically altered. The frequency of each alteration is shown. Frequency and footprint *P* values were generated in STAC.

reference gastric DNA sample taken from the same individual. Fragile sites FRA3B and FRA16D were selected for this study because, as noted above, the SNP genotyping analysis indicated that these were commonly deleted sites with small and consistent consensus regions of copy change; this allowed molecular analysis to be done with the minimum

number of PCR targets for qPCR and pyrosequencing (see Materials and Methods). As shown in Table 1, copy number loss was detected at FRA3B and FRA16D in 83.3% (15 of 18) and 40% (6 of 15) of cases, respectively. Copy number gain was detected at FRA3B in 11.1% (2 of 18) of patients tested. Of note, copy changes were just as

frequent in cases without dysplasia as in cases with a maximum diagnosis of indefinite for dysplasia (FRA3B, $P > 0.29$; FRA16D, $P > 0.44$). Pyrosequencing of SNPs spaced within FRA3B or FRA16D, compared with SNPs taken from flanking regions, was done in one to six biopsies per patient, based on availability. When multiple BE samples were analyzed, samples were taken at 2-cm intervals within the BE segment. LOH or AI was detected in at least one SNP and at least one BE biopsy within FRA3B in 75.0% (15 of 20) of patients (Table 1). At the FRA16D site, we detected LOH or AI in 70.0% of patients (14 of 20). These results confirm the high frequency of copy loss and LOH observed by whole genome analysis.

Loss at fragile sites detected in BE cell lines

To further validate these results, we tested for the extent of copy number losses at FRA3B and FRA16D in populations of BE cells grown in culture, cell lines CPA, CPB, CPC, and CPD (32, 33), on higher density Agilent 244K SNP arrays. Figure 2 shows copy number plots at two common fragile sites, FRA3B and FRA16D. Well-defined interstitial one- and two-copy deletions were present at FRA3B in all four cell lines tested, and moreover, in each case, at least two to four discrete one- or two-copy number loss events were visible. At FRA16D, two copy losses were flanked by regions of one copy number loss in CPA and CPC, whereas normal copy numbers were observed at the FRA16D locus in cell lines, CPB and CPD. A small region of copy number loss was also detected in two of four cell lines at FRA3C (data not shown).

Evolution of FRA3B instability over time

Having shown that copy loss at fragile sites was present at very high frequency in earlier molecular stages of this disease, we next asked whether a temporal and spatial analysis would reveal evolving instability within fragile sites in these patients. Endoscopic biopsies were examined from a single low-risk patient (without dysplasia, *p53*, DNA content tetraploidy, or aneuploidy) followed during surveillance (29) over a 16-year time span. Biopsies from three different levels, 26, 29, and 32 cm (± 1 cm) within a single BE segment, were analyzed using the Illumina Human-Hap300 BeadChips. Figure 3 illustrates the regions of greatest instability at FRA3B observed longitudinally at the 29-cm level. More than eight distinct copy loss events were seen within FRA3B/FHIT, seven of which were observed over a 4-year time span. Corresponding LOH was detected in regions of one-copy (but not two copy) loss (data not shown). Similar regions of one-copy loss were detected at the other levels in the regions of 60.3 to 60.35 Mb and 60.55 to 60.6 Mb on chromosome 3. Two-copy loss was detected in a 240-kb region from 60.33 to 60.57 Mb on this chromosome at all three levels at 1993. The copy loss event at 60.6 to 60.63 Mb appeared with less frequency—at 29/30 cm, two-copy loss was observed, but at 26 and 32 cm, one-copy loss was observed. This patient also had copy loss at other fragile sites (e.g., FRA16D and FRA7G), some of which showed additional

lesions over time (data not shown). Thus, in this patient, FRA3B clearly showed the greatest rate of change and evolution over time.

Discussion

Using SNP genotyping analysis to profile for LOH and copy number, with confirmation by quantitative PCR and pyrosequencing, we have shown that copy number alteration and/or LOH at chromosomal fragile sites are frequent and early events in BE neoplasia. Copy number loss and LOH was validated at FRA3B and FRA16D using PCR and pyrosequencing. Copy number loss at FRA3B is a particularly common early event, being observed in 80% of 20 early-stage endoscopic biopsies. The fragile site deletions that are reported were not observed in gastric samples from these patients, and thus, these abnormalities are not constitutional polymorphisms and are specific to the premalignant columnar BE tissue.

Although instability at fragile sites has been reported in several different cancers, this study shows high frequency of copy number loss and LOH within multiple defined regions associated with chromosomal fragile sites in a premalignant tissue. Fragile sites may be particularly sensitive to damage in Barrett's epithelium due to chronic acid exposure, which promotes an antiproliferative effect on Barrett's epithelium and increases stalling at the late replicating foci (38). Although trinucleotide repeat expansion has been reported as the mechanism for rare fragile site instability, recent data suggest that the distinctions between mechanisms of instability at common versus rare fragile sites are not so stringent, as aphidocolin-induced instability was observed at both common and rare fragile sites (39). We suggest that fragile site instability in BE may be similar in this regard.

It seems that regions of copy loss and LOH in BE can be narrow and well conserved, in at least in a subset of fragile sites, and this is most evident in BE at FRA3B. Although published studies of various cancers have reported deletions at FRA3B, these deletions range in size from 300 kb to over 2 Mb (40–42), and deletions consistently constrained to this specific subregion of FRA3B (60.2–60.6 MB, corresponding to FHIT exons 4–5) have not previously been reported in the literature. Both the high frequency and the uniformity of the alterations in BE may reflect a common etiology of genotoxic stress; in BE, this is likely oxidative damage, both as a direct effect of bile acids (15, 43, 44) and secondarily from oxygen and nitrogen-free radicals produced by inflammation. The primary, secondary, and tertiary structure of fragile sites is thought to promote stalling of DNA replication forks, which can induce recombination and strand breakage at fragile sites (45). If instability at fragile sites does indeed reflect the history of genotoxic stress in these patients, then it may serve as a biomarker of an individual's history of such damage (45). Importantly, breaks at fragile sites are induced by replication stresses *in vitro* (39, 46), suggesting that fragile sites may be the first regions of the genome to be mutated during chronic carcinogenic exposure *in vivo* (13). Our

data support the idea of a specific DNA damage profile, similar to asbestos-related lung cancer, in which a significant association between copy changes at 11 fragile sites (including FRA19B, FRA22A, and FRA11H) and asbestos-associated alterations by SNP genotyping has been reported (19).

Thus, measurement of deletion and LOH at fragile sites merits evaluation as a biomarker of cancer risk in BE patients. This biomarker could also play a role as an intermediate indicator of the success of chemopreventative strategies in BE. Such applications could include the use of nonsteroidal anti-inflammatory drugs, which reduce inflammation and are protective for development of EA (47), as well as long-term acid suppression, a common therapy for BE, which has been shown to decrease cellular proliferation through downregulation of *Mcm2* expression (48), and could potentially stabilize fragile sites by alleviating replicative stress.

There are several challenges to the development of robust assays that are sufficiently sensitive to detect rare sequences in a background of normal sequence: technical challenges in detecting rare sequences against a normal background and the challenge of defining a novel sequence in the target cells of interest. Although some genetic alterations have been reported to be present in premalignant BE tissue (2, 49-51), none have thus far been present at a sufficiently high frequency to enable their use in screening of at-risk populations. We have described a genetic lesion that is present in ~90% of early-stage BE. Therefore, this is a unique case in which we know in advance with ~90% sensitivity the identity of a DNA sequence abnormality in the

target cells, with the opportunity to increase this to ~100% by analysis of several additional fragile sites. With the exception of viral sequences (such as human papillomavirus in cervical cells), a genetic marker of preneoplastic cells has heretofore not been available for a premalignant tissue. Future expansion of these studies to include patients with the spectrum of disease progression and known outcomes would shed more light onto the prognostic value of this type of genomic instability in predicting development of dysplasia and cancer in BE.

Disclosure of Potential Conflicts of Interest

No potential conflicts of interest were disclosed.

Acknowledgments

We thank Jasmine Gallaher for the technical assistance and Biotage for use of the pyrosequencer. Illumina, BeadArray, and Infinium are registered trademarks or trademarks of Illumina, Inc. EVO and GenePaint are registered trademarks or trademarks of Tecan, AG.

Grant Support

NIH grants P01 CA91955 (P.S. Rabinovitch and C.C. Maley), 2 R44 CA103406-02 (K.L. Gunderson), and T32 AG00057 (L.A. Lai). C.C. Maley and R. Kostadinov were also supported in part by a PhRMA Foundation Informatics Research Starter Grant, the Pew Charitable Trust, and the Commonwealth Universal Research Enhancement Program from the Pennsylvania Department of Health.

The costs of publication of this article were defrayed in part by the payment of page charges. This article must therefore be hereby marked *advertisement* in accordance with 18 U.S.C. Section 1734 solely to indicate this fact.

Received 12/09/2009; revised 06/03/2010; accepted 07/06/2010; published OnlineFirst 07/20/2010.

References

- Jenkins GJ, Doak SH, Pary JM, et al. Genetic pathways involved in the progression of Barrett's metaplasia to adenocarcinoma. *Br J Surg* 2002;89:824-37.
- Sihvo EI, Salminen JT, Rantanen TK, et al. Oxidative stress has a role in malignant transformation in Barrett's oesophagus. *Int J Cancer* 2002;102:551-5.
- Wild CP, Hardie LJ. Reflux, Barrett's oesophagus and adenocarcinoma: burning questions. *Nat Rev Cancer* 2003;3:676-84.
- Morales TG, Sampliner RE. Barrett's esophagus: update on screening, surveillance, and treatment. *Arch Intern Med* 1999;159:1411-6.
- Nietert PJ, Silverstein MD, Mokhashi MS, et al. Cost-effectiveness of screening a population with chronic gastroesophageal reflux. *Gastrointest Endoscopy* 2003;57:311-8.
- Finley JC, Reid BJ, Odze RD, et al. Chromosomal instability in Barrett's esophagus is related to telomere shortening. *Cancer Epidemiol Biomarkers Prev* 2006;15:1451-7.
- O'Sullivan JN, Finley JC, Risques RA, et al. Telomere length assessment in tissue sections by quantitative FISH: image analysis algorithms. *Cytometry* 2004;58A:120-31.
- Lai LA, Paulson TG, Li X, et al. Increasing genomic instability during premalignant neoplastic progression revealed through high resolution array-CGH. *Genes Chromosomes Cancer* 2007;46:532-42.
- Michael D, Beer DG, Wilke CW, et al. Frequent deletions of FHIT and FRA3B in Barrett's metaplasia and esophageal adenocarcinomas. *Oncogene* 1997;15:1653-9.
- Fang JM, Arlt MF, Burgess AC, et al. Translocation breakpoints in FHIT and FRA3B in both homologs of chromosome 3 in an esophageal adenocarcinoma. *Genes Chromosomes Cancer* 2001;30:292-8.
- Yunis JJ, Soreng AL. Constitutive fragile sites and cancer. *Science* 1984;226:1199-204.
- Sutherland GR, Richards RI. The molecular basis of fragile sites in human chromosomes. *Curr Opin Genet Dev* 1995;5:323-7.
- Wang YH. Chromatin structure of human chromosomal fragile sites. *Cancer Lett* 2006;232:70-8.
- Schwartz M, Zlotorynski E, Kerem B. The molecular basis of common and rare fragile sites. *Cancer Lett* 2006;232:13-26.
- O'Keefe LV, Richards RI. Common chromosomal fragile sites and cancer: focus on FRA16D. *Cancer Lett* 2006;232:37-47.
- Arlt MF, Miller DE, Beer DG, et al. Molecular characterization of FRAXB and comparative common fragile site instability in cancer cells. *Genes Chromosomes Cancer* 2002;33:82-92.
- Ahmadian M, Wistuba II, Fong KM, et al. Analysis of the FHIT gene and FRA3B region in sporadic breast cancer, preneoplastic lesions, and familial breast cancer probands. *Cancer Res* 1997;57:3664-8.
- Fong KM, Biesterveld EJ, Virmani A, et al. FHIT and FRA3B 3p14.2 allele loss are common in lung cancer and preneoplastic bronchial lesions and are associated with cancer-related FHIT cDNA splicing aberrations. *Cancer Res* 1997;57:2256-67.
- Nymark P, Wikman H, Ruosaari S, et al. Identification of specific gene copy number changes in asbestos-related lung cancer. *Cancer Res* 2006;66:5737-43.
- Kuroki T, Tajima Y, Furui J, et al. Common fragile genes and digestive tract cancers. *Surg Today* 2006;36:1-5.
- Smith DI, Zhu Y, McAvoy S, et al. Common fragile sites, extremely large genes, neural development and cancer. *Cancer Lett* 2006;232:48-57.
- Hellman A, Zlotorynski E, Scherer SW, et al. A role for common

- fragile site induction in amplification of human oncogenes. *Cancer Cell* 2002;1:89–97.
23. Miller CT, Lin L, Casper AM, et al. Genomic amplification of MET with boundaries within fragile site FRA7G and upregulation of MET pathways in esophageal adenocarcinoma. *Oncogene* 2006;25:409–18.
 24. Ciullo M, Debily MA, Rozier L, et al. Initiation of the breakage-fusion-bridge mechanism through common fragile site activation in human breast cancer cells: the model of PIP gene duplication from a break at FRA7L. *Hum Mol Genet* 2002;11:2887–94.
 25. Feagins LA, Zhang HY, Hormi-Carver K, et al. Acid has antiproliferative effects in nonneoplastic Barrett's epithelial cells. *Am J Gastroenterol* 2007;102:10–20.
 26. Zhang HY, Zhang X, Hormi-Carver K, et al. In non-neoplastic Barrett's epithelial cells, acid exerts early antiproliferative effects through activation of the Chk2 pathway. *Cancer Res* 2007;67:8580–7.
 27. Hong MK, Laskin WB, Herman BE, et al. Expansion of the Ki-67 proliferative compartment correlates with degree of dysplasia in Barrett's esophagus. *Cancer* 1995;75:423–9.
 28. Reid BJ, Sanchez CA, Blount PL, et al. Barrett's Esophagus - Cell cycle abnormalities in advancing stages of neoplastic progression. *Gastroenterology* 1993;105:119–29.
 29. Reid BJ, Blount PL, Rubin CE, et al. Flow-cytometric and histological progression to malignancy in Barrett's esophagus: prospective endoscopic surveillance of a cohort. *Gastroenterology* 1992;102:1212–9.
 30. Galipeau PC, Li XH, Blount PL, et al. NSAIDs modulate CDKN2A, TP53, and DNA content risk for progression to esophageal adenocarcinoma. *Plos Med* 2007;4:342–54.
 31. Paulson TG, Galipeau PC, Reid BJ. Loss of heterozygosity analysis using whole genome amplification, cell sorting, and fluorescence-based PCR. *Genome Res* 1999;9:482–91.
 32. Palanca-Wessels MC, Barrett MT, Galipeau PC, et al. Genetic analysis of long-term Barrett's esophagus epithelial cultures exhibiting cytogenetic and ploidy abnormalities. *Gastroenterology* 1998;114:295–304.
 33. Palanca-Wessels MC, Klingelhutz A, Reid BJ, et al. Extended lifespan of Barrett's esophagus epithelium transduced with the human telomerase catalytic subunit: a useful *in vitro* model. *Carcinogenesis* 2003;24:1183–90.
 34. Peiffer DA, Le JM, Steemers FJ, et al. High-resolution genomic profiling of chromosomal aberrations using Infinium whole-genome genotyping. *Genome Res* 2006;16:1136–48.
 35. Wang P, Kim Y, Pollack J, et al. A method for calling gains and losses in array CGH data. *Biostatistics* 2005;6:45–58.
 36. Diskin SJ, Eck T, Greshock J, et al. STAC: a method for testing the significance of DNA copy number aberrations across multiple array-CGH experiments. *Genome Res* 2006;16:1149–58.
 37. Boehm D, Herold S, Kuechler A, et al. Rapid detection of subtelomeric deletion/duplication by novel real-time quantitative PCR using SYBR-green dye. *Hum Mutat* 2004;23:368–78.
 38. Feagins LA, Zhang HY, Quinones M, et al. Acid exerts an anti-proliferative effect in non-neoplastic Barrett's epithelial cells by delaying cell cycle progression. *Gastroenterology* 2006;130:A77.
 39. Mrasek K, Schoder C, Teichmann AC, et al. Global screening and extended nomenclature for 230 aphidicolin-inducible fragile sites, including 61 yet unreported ones. *Int J Oncol* 2010;36:929–40.
 40. Lisitsyn NA, Lisitsina NM, Dalbagni G, et al. Comparative genomic analysis of tumors: detection of DNA losses and amplification. *Proc Natl Acad Sci U S A* 1995;92:151–5.
 41. Kameoka Y, Tagawa H, Tsuzuki S, et al. Contig array CGH at 3p14.2 points to the FRA3B/FHIT common fragile region as the target gene in diffuse large B-cell lymphoma. *Oncogene* 2004;23:9148–54.
 42. Huebner K, Garrison PN, Barnes LD, et al. The role of the FHIT/FRA3B locus in cancer. *Annu Rev Genet* 1998;32:7–31.
 43. Jenkins GJ, D'Souza FR, Suzen HS, et al. Deoxycholic acid (DCA) at neutral and acid pH, is genotoxic to oesophageal cells through the induction of ROS: the potential role of antioxidants in Barrett's oesophagus. *Carcinogenesis* 2007;28:136–42.
 44. Payne CM, Weber C, Crowley-Skillicorn C, et al. Deoxycholate induces mitochondrial oxidative stress and activates NF- κ B through multiple mechanisms in HCT-116 colon epithelial cells. *Carcinogenesis* 2007;28:215–22.
 45. Glover TW, Arlt MF, Casper AM, et al. Mechanisms of common fragile site instability. *Hum Mol Genet* 2005;14:R197–205.
 46. Durkin SG, Ragland RL, Arlt MF, et al. Replication stress induces tumor-like microdeletions in FHIT/FRA3B. *Proc Natl Acad Sci U S A* 2008;105:246–51.
 47. Vaughan TL, Dong LM, Blount PL, et al. Non-steroidal anti-inflammatory drugs and risk of neoplastic progression in Barrett's oesophagus: a prospective study. *Lancet Oncol* 2005;6:945–52.
 48. Lao-Sirieix P, Roy A, Worrall C, et al. Effect of acid suppression on molecular predictors for esophageal cancer. *Cancer Epidemiol Biomarkers Prev* 2006;15:288–93.
 49. Galipeau PC, Prevo LJ, Sanchez CA, et al. Clonal expansion and loss of heterozygosity at chromosomes 9p and 17p in pre-malignant esophageal (Barrett's) tissue. *J Natl Cancer Inst* 1999;91:2087–95.
 50. Gonzalez MV, Artimez ML, Rodrigo L, et al. Mutation analysis of the p53, APC, and p16 genes in the Barrett's oesophagus, dysplasia, and adenocarcinoma. *J Clin Pathol* 1997;50:212–7.
 51. Koppert LB, Wijnhoven BP, van Dekken H, et al. The molecular biology of esophageal adenocarcinoma. *J Surg Oncol* 2005;92:169–90.